Design of the Series Hybrid Reconfiguration of a General Aviation Aircraft *

L. Trainelli, M. Anselmi, M. Ballarin, S. D'Andrea,[a] G. Zuliani[b]

[a]Dipartimento di Scienze e Tecnologie Aerospaziali, Politecnico di Milano, Milano, Italy

[b]Technoline Engineering SA, Ruvigliana, Switzerland

Nomenclature

c_P	=	thermal engine specific fuel consumption
e	=	endurance and range function (eq. 10)
f	=	weight function (eq. 6)
g	=	gravity field intensity
k	=	thermal engine power drop-off exponent
k_P	=	battery Peukert exponent
t_d	=	battery discharge time
C_c	=	battery nominal charge rate
C_d	=	battery nominal discharge rate
C_D	=	drag coefficient
C_L	=	lift coefficient
H_b	=	full charge battery energy
I_c	=	battery input current
I_d	=	battery discharge current
I_{nom}	=	battery nominal discharge current
K_t	=	endurance and range constant (eq. 9)
P	=	electric motor installed power
P_a	=	available power for flight
P_c	=	battery charging power
P_r	=	required power for flight
P_t	=	thermal engine output power
S	=	wing reference surface
V	=	true airspeed
V_m	=	electric motor voltage
V_H	=	maximum airspeed in steady level flight
W	=	gross weight
$\mathcal{E}$	=	endurance
$\mathcal{R}$	=	range
η	=	overall mode efficiency
η_b	=	battery efficiency
η_g	=	electric generator efficiency
η_h	=	total hybrid system efficiency
η_i	=	inverter efficiency
η_m	=	electric motor efficiency
η_p	=	propeller efficiency
η_t	=	thermal engine efficiency
μ	=	runway rolling friction coefficient
ρ	=	air density

Acronyms

CG	=	centre of gravity
GA	=	General Aviation
ICE	=	internal combustion engine
MTOW	=	maximum take-off weight

*Based on a paper presented at the XXII Congresso Nazionale AIDAA - Associazione Italiana di Aeronautica e Astronautica, September 2013, Napoli, Italia

1. Introduction

The binding need in the reduction of the environmental impact of aviation is leading towards an increasing interest in the design of more sustainable products and systems for various classes of aircraft. The wider adoption of electric power systems is bene-

ficial with respect to emissions of CO_2, NO_x and other contaminants, as well as to noise pollution. Also, operative cost reduction can be expected, as well as a lower dependence on fossil fuel price fluctuations.

The General Aviation (GA) market is no exception. In fact, while the global number of GA airplanes is substantially less than the number of commercial airplanes, and the same would be of the number of airplanes involved in this innovation process, the widespread territorial diffusion of light aviation and the shorter time-to-market of innovative applications may represent strong points for boosting innovation. Furthermore, the relative simplicity of light aircraft systems allows to pursue research projects in this field with relatively limited resources and a faster development and testing process.

Contrary to some other experiences in the field of light aviation (Yuneec International E430, Pipistrel Taurus Electro G2, Lange Aviation Antares 20E), we do not consider pure electric propulsive configurations, *i.e.* where the only source of energy on board is represented by the battery packs. Indeed, due to the current technology limitations concerning energy and power density of available battery cells, these applications inevitable suffer from significant range and endurance restrictions if satisfactory point performance have to be preserved. Therefore, the possibility of a wide diffusion in the GA at large is unlikely, at least in the near future. On the other hand, a hybrid propulsion system seems to have the potential for widespread usage, allowing to achieve adequate point and integral performance while offering the possibility to attain enhanced safety, higher internal comfort, lower vibration levels, a reduced noise signature, and emission abatement with respect to conventional airplanes in the same class.

Two basic architectures can be considered, the "parallel hybrid" and the "series hybrid". The first associates a conventional aeronautical internal combustion engine (ICE) with a an electric motor, both driving the propeller shaft. This allows diverse design concepts to be developed, such as the case in which the ICE is sized to the relatively low power requirement fro cruise, while the electric motor provides the extra power needed for take-off and climb, adding at the same time the opportunity of a residual power in case of ICE failure. An example of a future, innovative parallel hybrid application is given in [1].

Here we consider a series, or "serial", reconfiguration (Figure 1), where the native propulsive system, *i.e.* a conventional aeronautical ICE, is replaced with a system composed of an electric motor directly connected to the propeller, and by an existing ICE currently employed in automotive applications. This arrangement provides a high level of safety and reliability, while insuring a substantial noise reduction, especially in terminal operations, and even possible fuel savings connected to optimized steady-state working

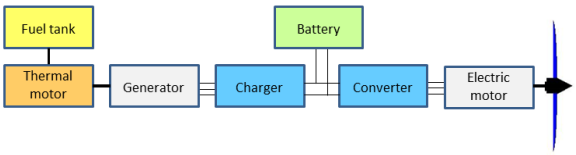

Figure 1. Series hybrid architecture.

conditions of the system. In this architecture, the ICE, coupled with an electric generator, acts both as the power source for the electric motor and as an in-flight recharger for the battery pack ("range extender" concept, currently employed in some automotive applications). This entails that two operating conditions are available: a "hybrid mode" where the ICE/generator subsystem provides the electric power necessary both to the electric motor and to the recharge of the battery pack; and a "pure electric mode", where the ICE is shut off and the electric motor is fed by the discharge of the battery pack.

The discussed configuration is at variance with respect to two previous examples of hybrid airplanes developed in recent years: the ENFICA-FC first flown in 2007 [2] and the SkySpark first flown in 2009 [3]. These demonstrators were both powered by "fuel-cell hybrid" systems, where the batteries are recharged by hydrogen fuel cells. The latter's development was stopped before reaching complete onboard integration, but was capable to achieve the world record for maximum airspeed as a pure electric aircraft in 2009, reaching a top speed of 136 kn. Both programs were based on the reconfiguration of existing low-wing, conventional ultralight airplanes. They represent highly valuable research achievements, but seem to be still far from a widespread practical application, mainly because of the complexity of the fuel cell system.

A different approach has been pursued in the Eco-Eagle project flown in 2011 [4], based on a modified Stemme S-10 motor glider, powered by a combination of a high power ICE and a lower power eletric motor. In this 'parallel' system, the two power sources are alternative to each other, with the ICE operating in take-off and climb high power regimes, switching to the electric motor in low power cruise conditions. Albeit a remarkable achievement, the Eco-Eagle also appears as a pioneering application, open to further development and optimization.

Another significant accomplishment exploiting the favorable low drag characteristics of gliders is the Dimona E-Star first flown in 2011, powered by a serial hybrid drive [5] based on a Wankel-type rotary ICE. This project is based on the reconfiguration of a HK36 Super Dimona low-wing, T-tailed, two-seat motor glider.

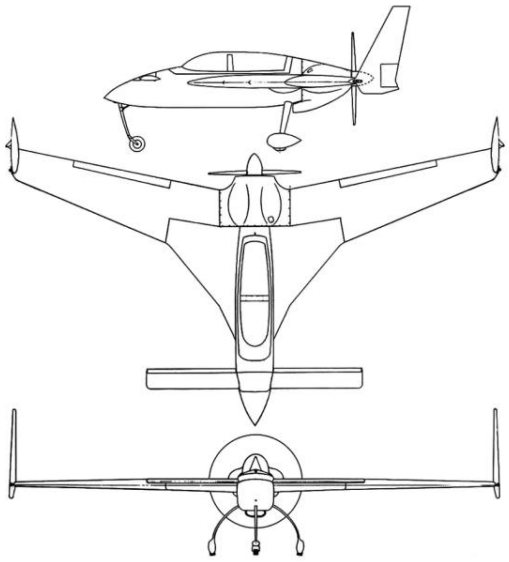

Figure 2. Three-view of the Rutan Model 61 Long-EZ experimental category airplane.

Table 1
Rutan Model 61 Long-EZ data

Wing span	7.90 m
Wing surface	7.62 m^2
Length	5.12 m
Height	2.40 m
Canard empennage span	3.60 m
Canard empennage surface	1.19 m^2
Max take-off weight (MTOW)	601 kg_p
Empty weight	340 kg_p
Fuel tank capacity	197 l
Power installed	86 kW
Max cruising speed	160 kn
Crusing speed	125 kn
Range	3,200 km
Service ceiling	27,000 ft
Rate of climb	1,750 ft/min

Cruise performance vouch for an optimum airspeed of 98 kn, a never exceed airspeed of 148 kn and maximum range of 1094 km.

2. Project Description

The present project has been initiated at the Department of Aerospace Science and Technology of the Politecnico di Milano [6,7], starting from an idea of G. Zuliani, amateur builder and owner/operator of a Rutan Model 61 Long-EZ (Figure 2). This homebuilt airplane has a canard, two-seater, pusher-propeller configuration. It features a Maximum Take-Off Weight (MTOW) of 601 kg_p and is typically powered by a reciprocating engine in the 100∼115 HP range. Other characteristics are shown in Table 1.

The Long-EZ is widely considered a very aerodynamically efficient airplane, with remarkable speed and range performance. These characteristics, along with the wide space available in the fuselage where the engine is installed, larger than in typical tractor-propeller airplanes of the same class, provide an ideal ground for the present research effort. Also, since the Long-EZ belongs to the experimental category (*i.e.* homebuilt aircraft), a possible prototypal realization to be employed as a research test-bed and technology demonstrator is made much easier than with any aircraft in a certified category. Incidentally, a recent development that achieved the speed record for a man carrying electric powered aircraft in level flight, is the "Long ESA", *i.e.* a Long-EZ reconfigured with an exuberant 210 kW electric engine that adventurously broke the 200 mph (173 kn) barrier in July 2012, performing a 'deadstick' landing after completely losing residual onboard power [8].

Based on the above discussion, the present project aims to produce a relatively simple, albeit high-performance and captivating, single-seat demonstrator for the series hybrid architecture, in view of a future implementation capable to retain the possibility of embarking a passenger. In fact, as a challenging start, we placed strict requirements in terms of MTOW preservation allowing for the passenger seat to be disembarked and its space exploited for accommodating the batteries and other components of the new propulsive system. Furthermore, we required to achieve minimal impact on the existing airframe and minimal effects upon the original aircraft handling qualities.

In addition, we considered the possibility of establishing FAI (Fédération Aéronautique Internationale) records with respect to airspeed (aiming to a lower value than the pure-electric Long-ESA, but within a more reliable setup), time to climb, and range. In particular, we set the following performance goals:

- Performance Goal 1: maximum airspeed at altitude of 8000 ft, aiming to 160 kn;
- Performance Goal 2: climb up to 20,000 ft in less than 20 minutes;
- Performance Goal 3: maximum range with 80 l of fuel on board, aiming to 2000 km.

Translating these goals into performance specifications led to installed energy and power requirements, which in turn triggered the sizing of the electric motor, the battery pack, the ICE, the generator, and the other components. The battery pack proves to be the most critical element, being characterized by

Table 2
Typical component efficiencies

Generator	$\eta_g = 0.85$
Charger	$\eta_{i_1} = 0.90$
Battery pack	$\eta_b = 0.90$
Converter	$\eta_{i_2} = 0.90$
Electric motor	$\eta_m = 0.85$

technology limitations concerning energy density and charge/discharge behaviour. Nevertheless, we were able to prove the feasibility of the project and the promising improvements in sustainability, highlighting strong and weak points, as well as important criticalities.

3. Series Configuration

The proposed hybrid system, following the scheme depicted in Figure 1, consists in the coupling of an ICE of efficiency η_t with an electric generator of efficiency η_g that recharges the batteries of efficiency η_b through a first inverter (charger) of efficiency η_{i_1}; the batteries then power the electric motor of efficiency η_m through a second inverter (converter) of efficiency η_{i_2}; the electric motor finally actuates the propeller of efficiency η_p. A conservative estimate of the efficiency values for the electric components, used in the following calculations, is given in Table 2.

We assume a value $\eta_t = 0.35$ for the ICE to be installed. This value appears reasonable for a modern, optimized engine, such as those currently installed on the automobiles of the latest generation, working at its best efficiency conditions. This clearly represents a significant improvement over the average efficiencies of existing ICE employed in GA applications, for which a maximum value may reach $\eta_t = 0.25$ at best.

4. Energy Analysis

We consider now the energy required to perform the three mission goals stated in the Introduction, including in addition the take-off manoeuvre. The purpose of this analysis is to provide significant data for the sizing of the hybrid system and to identify the critical operating conditions. Energy required to accomplish the mission tasks is computed as a function of the electric motor installed power. All mission tasks are considered assuming that the starting aircraft weight is the MTOW of the original aircraft (601 $\mathrm{kg_p}$).

4.1. Take-off

A standard analysis for the take-off procedure based on the FAR/CS-23 definitions [9] has been performed to determine the dependence of the energy required to accomplish the manoeuvre on the electric motor installed power P. We considered a ground run phase and an airborne phase up to 50 ft above ground level. Under customary hypothesis, involving a constant friction coefficient $\mu = 0.25$, a constant propeller efficiency $\eta_p = 0.28$, constant optimal lift and drag coefficients $C_L = 0.35$ and $C_D = 0.027$, we obtained a complete parameterization of take-off performance specifications such as ground run distance (Figure 3a) and energy required (Figure 3b). The ground run distance should be compared to typical values of 300∼350 m, retrieved from information available and actually verified by one of the co-authors in his own operational use of the Long-EZ.

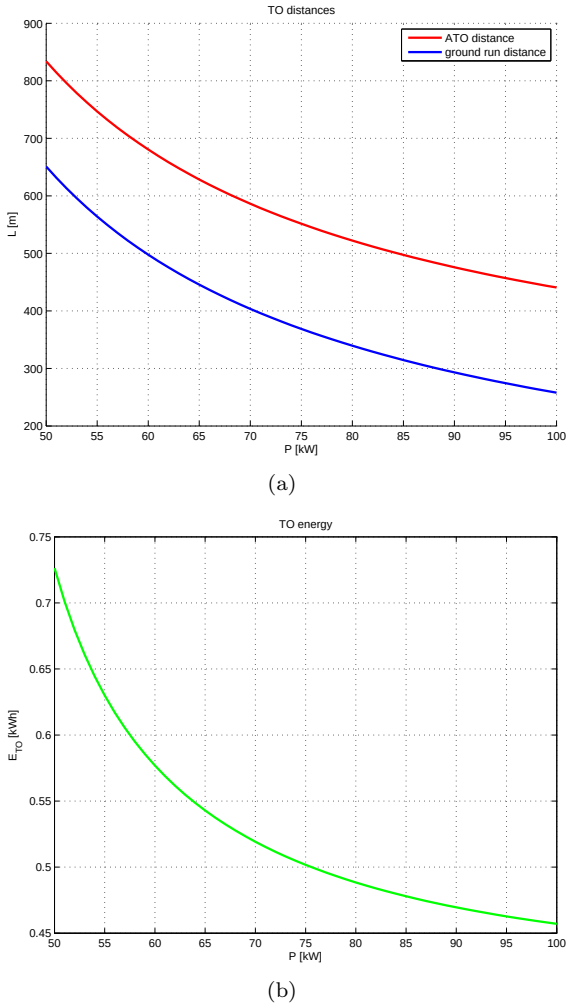

Figure 3. (a) Ground run distance (blue) and total critical (aborted take-off) distance. (b) Energy required to complete take-off. Both are drawn as functions of electric motor installed power.

4.2. Performance Goal 1: Maximum airspeed

We consider the energy required to reach the maximum airspeed at 8,000 ft altitude, and to maintain this

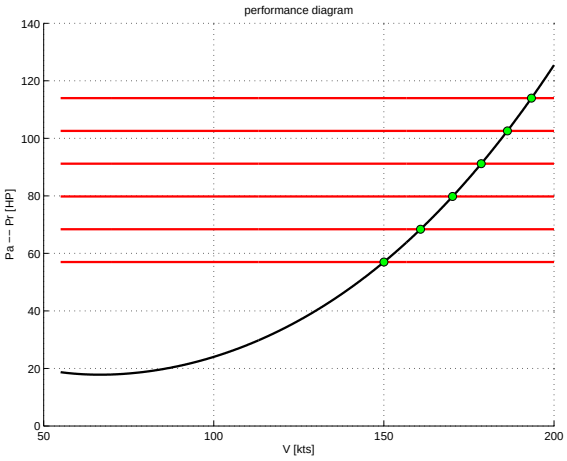

Figure 4. Power available (red) and power required at 8,000 ft, as functions of true airspeed.

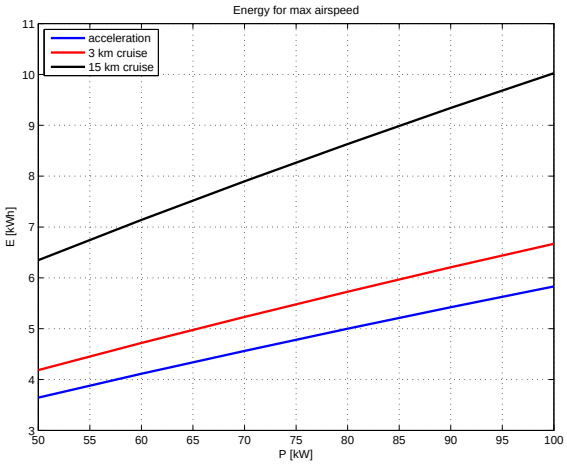

Figure 5. Energy required to reach (blue) and maintain maximum airspeed for 3 km (red) and 15 km (black) as a function of electric motor installed power.

condition on a horizontal distance of 3 km and 15 km. We assume the mission to be performed in all-electric mode, with constant weight and constant power, and consider horizontal flight (in place of a less demanding descending flight). The maximum airspeed V_H is retrieved as a function of available power through the level flight equilibrium conditions, as shown in the classical Pénaud power performance diagram (Figure 4). The energy required for the first performance goal item, acceleration to V_H, has been computed integrating the acceleration $\dot{V}$ retrieved from the longitudinal equation of motion as

$$\dot{V} = \frac{g}{V}\frac{P_a - P_r}{W}, \tag{1}$$

where $P_a = \eta_p P$ denotes power available, and P_r power required. The acceleration manoeuvre is assumed to start from a trimmed condition at the minimum drag airspeed, which amounts to 88 kn at 8,000 ft. This procedure allows to determine distance and time to maximum airspeed, as well as energy required. After reaching V_H, the energy required to maintain trim condition at this airspeed is computed, up to a distance flown of 3 and 15 km. Figure 5 shows these energy values as functions of installed power P.

4.3. Performance Goal 2: Time to climb

We consider the energy required to reach 20,000 ft altitude from sea level, aiming to a climb time not exceeding 20 min. The climb profile is assumed to follow a 'traditional' fastest climb program, *i.e.* flying at the minimum power required airspeed. This, for a constant rpm, variable pitch propeller, ICE-powered aircraft represents also an optimal or nearly-optimal economic climb. In this case, as a first guess, we assume that the difference arising from the different motorization is not substantial. We assume the climb to be performed in hybrid mode, with constant power and a SFC (specific fuel consumption) of 0.35 lbf/hp/hr. The assumed propeller efficiency value is $\eta_p = 0.80$.

Time, distance and fuel weight to climb have been computed by integrating the equations of motion under the customary assumptions of steady climb, accounting for fuel consumption. As an example, the relation between altitude and time to climb is presented in Figure 6, corresponding to different values of installed power P. The time necessary to reach 20,000

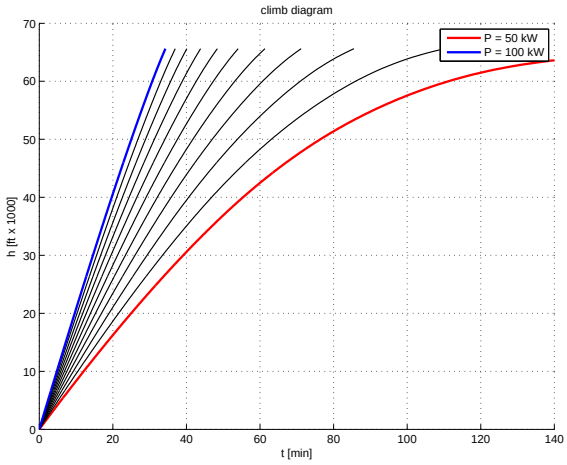

Figure 6. Altitude vs. time to climb, as a function of different values of electric motor installed power.

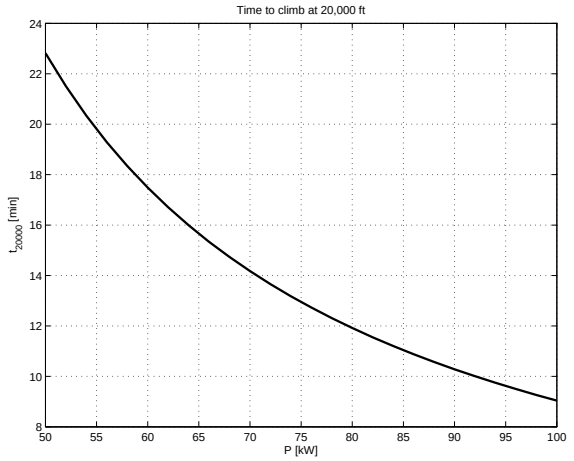

(a)

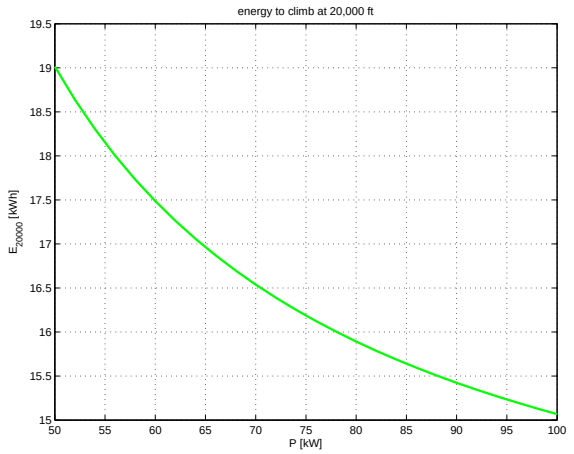

(b)

Figure 7. (a) Time to climb up to 20,000 ft. (b) Energy required to climb up to 20,000 ft. Both are drawn as functions of electric motor installed power.

ft is depicted as a function of installed power P in Figure 7a, while the energy required for this performance goal is shown in Figure 7b.

4.4. Performance Goal 3: Maximum range

In this case, we seek the range performance given a fixed value of the energy stored on board. This energy corresponds to the maximum amount of fuel usable, amounting to 80 l. In order to optimize energy resources, we adopt an energy management based on a "start and stop" strategy for the ICE. Therefore, the cruise will be composed of alternating segments conducted in "pure electric mode" (mode A) and "hybrid mode" (mode B).

In pure electric mode, batteries drive the electric motor from full charge until a prescribed discharge level is reached, and the ICE is kept off. Therefore weight is kept constant and the optimal cruise program involves constant airspeed, lift coefficient and altitude.

In hybrid mode, the ICE is switched on at (constant) maximum efficiency regime, to feed the electric motor. While cruising in hybrid mode, the ICE power is always higher than the power required to drive the electric motor, therefore excess power can be exploited to recharge the battery pack. Due to fuel consumption, weight decreases during this cruise segment and the optimal cruise program is the so-called "cruise-climb", where airspeed and lift coefficient are constant, while altitude slowly increases. This entails that power required decreases along the flight path, requiring adequate adjustment of the power output of the electric motor. When the batteries reach full charge, operations switch from hybrid mode to pure electric mode, and the process is repeated.

In the following, we address endurance and range calculation methods for the two operational modes.

4.4.1. Pure Electric Mode (A)

In this mode, power required by the electric motor is provided by the batteries, characterized by a full charge energy value H_b. Therefore, at constant weight, airspeed and altitude, endurance $\mathcal{E}^A$ and range $\mathcal{R}^A$ are given by

$$\mathcal{E}^A = \eta^A \frac{H_b}{P_r}, \tag{2}$$

$$\mathcal{R}^A = V\,\mathcal{E}^A = \eta^A V\,\frac{H_b}{P_r}, \tag{3}$$

where $\eta^A := \eta_b \eta_{i2} \eta_m \eta_p$ is the total efficiency in mode A. For the present application, we assume that the endurance equals the battery discharge time corresponding to the actual power request up to 80% discharge, leaving a residual 20% charge for safety reasons and to avoid excessive cycle stress on batteries.

4.4.2. Hybrid Mode (B)

In this mode, the power generated by the ICE is divided in two contributions, one driving the electric motor and the other recharging the batteries. Therefore, the time needed to fully recharge the batteries is retrieved by integrating the equation that equates the battery rate of charge $\dot{H}_b^c$ with the portion of the ICE power output in excess with respect to power required:

$$\dot{H}_b^c = \eta_{i1} \eta_b \left(\eta_g P_t - \frac{P_r}{\eta_m \eta_p} \right). \tag{4}$$

Both required power P_r and ICE power P_t are not constant during this flight mode. In fact, Since weight lessens during flight, P_r also reduces at constant airspeed and lift coefficient. Also, we assume a typical altitude drop-off law for the ICE power P_t as

$$P_t = \left(\frac{\rho}{\rho_{\text{ref}}} \right)^{(1+k)} P_{t_{\text{ref}}}, \tag{5}$$

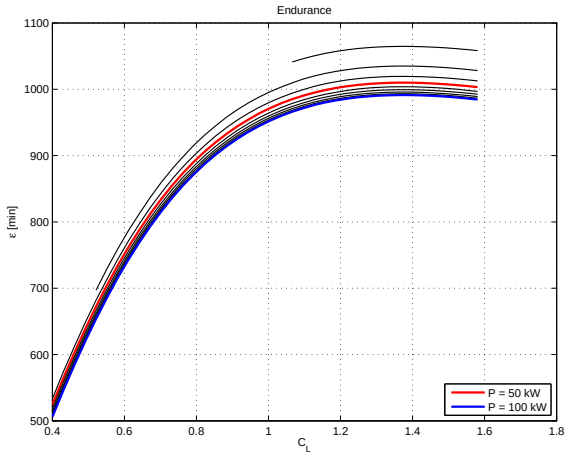

(a)

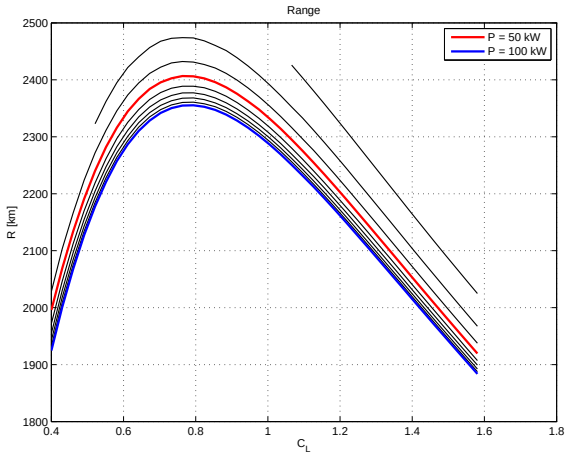

(b)

Figure 8. (a) Endurance. (b) Range. Both are drawn as functions of the cruise lift coefficient for different values of electric motor installed power.

where the reference altitude can be sea-level, in the case of an aspirated engine, or the critical altitude, for a supercharged engine. Integrating the previous equation leads to the following relationship

$$W_2 = f(W_1|H_b, C_L) \tag{6}$$

for the final weight W_2 corresponding to full battery recharge as a function of the segment initial weight W_1 and further parameterized in terms of battery charge H_b and cruise lift coefficient C_L. This leads to the following functions for endurance and range, involving the same variables:

$$\begin{aligned} \mathcal{E}^B &= \mathcal{E}^B(W_1|H_b, C_L) \\ &= \frac{1}{c_P K_t}\big(e(W_1) - e(W_2)\big), \end{aligned} \tag{7}$$

$$\begin{aligned} \mathcal{R}^B &= \mathcal{R}^B(W_1|H_b, C_L) \\ &= \frac{1}{c_P K_t}\sqrt{\frac{2}{\rho_1}\frac{W_1}{S}}\frac{e(W_1) - e(W_2)\big)}{\sqrt{C_L}} \end{aligned} \tag{8}$$

In the previous equations, c_P represents the ICE SFC, K_t is a constant defined by

$$K_t := \frac{P_{t_{\text{ref}}}}{\left(\frac{\rho_{\text{ref}}}{\rho_1} W_1\right)^{(1+k)}}, \tag{9}$$

while $e(W)$ is a function that depends on the ICE drop-off exponent k,

$$e(W) = \begin{cases} \log(W), & \text{if } k = 0 \\ -\frac{W^{-k}}{k}, & \text{if } k \neq 0 \end{cases}. \tag{10}$$

The details of this analysis are reported in [6, 7, 10].

Figure 8 shows the optimal endurance and range resulting from different installed power P values, as functions of the cruise lift coefficient.

5. Power System Sizing, Selection and Layout

The previous analysis allowed to gather the information necessary to the sizing of the hybrid power system, under the constraint of a total aicraft weight not higher than the Long-EZ design MTOW. An overview of the main features and performance of the main subsystems that were chosen to generate flight power are discussed hereafter.

5.1. Electric Motor

According to the results obtained in performance goal analysis, electric motor power should be in the range from 50 to 70 kW. This is a power target rarely associated to a low motor weight. An analysis of the current market options led to selecting the two COTS (commercial off-the-shelf) motors reported in Table 3 as the best candidates for the present application.

A distinctive advantage of both solutions lies in the possibility of direct drive connection to the propeller, without the need for a rpm reduction gear. The final choice fell on the "Va-lentino" by Sicmemotori,

Table 3
Main features of two candidate COTS electric motors

Manufacurer	Sicmemotori	Yuneec Int.
Model	Va-lentino	Power drive 60
Type	Brushless direct drive	Brushless direct drive
Max power [kW]	67.5	60
Speed [rpm]	2,500	2,400
Size [mm]	250×280	280×209
Voltage [V]	450	190
Current [A]	150	220
Weight [kg_p]	40	30

Table 4
Main features of Kokam batteries cell types adequate for take-off

Type	H_b [Ah]	W [g_p]	ρ_E $\left[\frac{\text{Wh}}{\text{kg}}\right]$	ΔV_m [V]	C_d [A]
1	12	345	129	3.69	15
2	31	780	147	3.69	8
3	13	325	148	3.69	8
4	25	560	165	3.70	5

mainly because of the higher values of power and voltage, the latter being exploited in battery sizing. The "Va-lentino" is a synchronous brushless electric motor with Neodymium-Iron-Boron permanent magnets. Low weight is a consequence of its external rotor configuration and high number of poles. This particular motor has been used in the SkySpark program [3].

5.2. Battery Pack

Battery pack is crucial to the power system sizing, heavily impacting on all aspects of the design, from aircraft weight to sizing of all the remaining electric and mechanical components. Battery weight depends on required energy, which is provided by mission requirements, and energy density, which is a characteristic of the chosen battery technology.

Concerning energy, we placed a severe requirement assuming a pure electric take-off as the sizing mission task. This seems interesting in view of the public acceptance of airport operations, given the significant reduction in the airplane noise signature when the ICE is shut off. However, it also amounts to a heavy constraint on the battery pack, since it corresponds to maximum power required and therefore, to maximum battery discharge rate. The analysis of battery performance included the Peukert effect, which represents the degradation of the battery cell capacity when a higher-than-nominal current value is requested [11]. Considering the voltage V_m of the chosen electric motor, the discharge current I_d necessary to the mission task is

$$I_d = \frac{P_r}{V_m}. \tag{11}$$

To guarantee that the batteries could supply the requested current, the following constraint was imposed:

$$I_d \leq I_{d_{\max}} := \frac{C_d}{I_{\text{nom}}}. \tag{12}$$

where $I_{d_{\max}}$ represents the maximum current output, I_{nom} the current corresponding to a 1-hour long discharge of the nominal cell capacity and the nominal discharge rate (*C-rate*) C_d indicates a characteristic parameter of each specific cell type.

Thirty different Li-Fe-Po battery cell types among the vast array marketed by Kokam were considered. For those which satisfied the previous constraint, discharge time t_d was evaluated according to the Peukert formula:

$$t_d = t_{\text{ref}} \left(\frac{H_b}{I_d\, t_{\text{ref}}} \right)^{k_P}, \tag{13}$$

where t_{ref} is the cell reference discharge time (normally equal to 10 or 20 hrs) and k_P is the Peukert exponent, assumed equal to 1.3 in the present case [11].

Battery types with discharge times higher or equal to mission task time were singled out: Type 1 (corresponds to the SLPB70205130P cell model) and Type 2 (SLPB78216216H) were found compliant to the set requirements, with features reported in Table 4, where W stands for cell weight, ρ_E for specific energy (or gravimetric energy density), and ΔV_m for cell nominal voltage.

A similar analysis was also carried out for a hybrid take-off procedure. In this case, ICE power was assumed in a range from 30 to 70 kW, evaluating the power fraction required for flight and the remaining part that can be used to recharge the batteries. Figure 9 shows the results of this study, under the assumption of a supercharged ICE, *i.e.* such that ICE power output is independent of altitude. In this figure, for each value of ICE power, the lower curve corresponds to sea level, and the higher one to an altitude of 20,000 ft. The horizontal lines represent the power necessary for different cell types and are retrieved on the base of the following relations:

$$P_{c_{\max}} = V_m I_{c_{\max}} = V_m C_c H_b, \tag{14}$$

where $P_{c_{\max}}$ indicates the maximum battery charging power, $I_{c_{\max}}$ the maximum battery input current, and

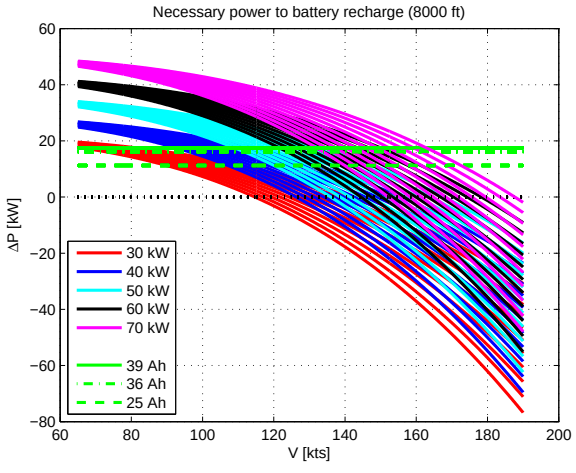

Figure 9. Power fraction necessary to recharge the batteries as a function of airspeed.

Table 5
Main features of selected automotive ICE

Manufacturer	VW	Smart
Type	TDI	Gasoline (turbo)
Cubic capacity [l]	1.2	1.0
Max power [kW]	56	62
Rpm for max power	4,200	5,250
Max torque [Nm]	180	120
Rpm for max torque	2,000	3,250
Optimum power [kW]	37	41
Consumption [l/100 km]	3.0	4.2
Emissions [CO2 g/km]	87	116

C_c the characteristic charge 'C-rate'. The cells individuated as appropriate in this condition are Type 1 (SLPB70205130P), Type 3 (SLPB60205130H) and Type 4 (SLPB60216216) reported in Table 4.

Focusing on an airspeed range from 90 to 120 kn, which correspond to usual cruise condition for the Long-EZ, led to the choice of an ICE installed power of 40 kW, insuring adequate recharging power during cruise. By evaluating the time necessary for battery recharge, accounting for the ICE power previously defined and the manufacturer's recharge data, two different types of battery cells have finally been selected: Types 1 and 2, both assembled to give a battery pack made up by 122 cells with a serial connection. Type 1, with a cell capacity of 12 Ah, was chosen mainly for the lower battery pack weight (45 kg_p). Type 2, with a cell capacity of 31 Ah, is definitely superior in term of energy performance, but at the expense of a higher battery pack weight (95 kg_p).

5.3. Internal Combustion Engine

ICE power sizing, as seen above, is closely connected to the power necessary for recharging the chosen battery packs. The ICE design condition, i.e. maximum efficiency, should meet a supply requirement of about 40 kW at 8,000 ft. On this ground, an analysis of the market opportunities was performed, ending up with two possible solutions, with specifications reported in Table 5. Among these, the Smart engine was eventually selected, because of smaller size and higher power available. Furthermore, it is a turbocharged engine, which allows to consider constant power output irrespective to flying altitude up to about 8,000 ft, and a progressive reduction up to 10∼15% at 20,000 ft.

5.4. Final layout

The completion of the propulsive system sizing has been performed considering the electric generator and the power inverters, as well as the cooling system. The power of the generator must match that of the ICE, therefore a possible choice is identified in another product of Sicmemotori, a brushless machine rated for 40 kW at 6000 rpm. Concerning the inverters, conventional COTS components are generally inadequate to the present application due to weight and volume tight requirements. Therefore, we selected the KERS (Kinetic Energy Recovery System) control unit by Magneti Marelli Sport already used in the SkySpark program [3], which guarantees adequate size and performance characteristics.

Table 6
Reconfigured weight breakdown

Item	[kg_p]
Original EOW	331
Native ICE LY-0235	−113
Pilot	85
Oil & liquids	6
Fuel	65
ICE	95
Generator	30
AC/DC inverter	5
Battery pack	45
DC/AC inverter	5
Electric motor	40
12V battery	3
DC/DC converter	2
TOW	599

The resulting weight breakdown is shown in Table 6, starting from the original EOW (empty operative weight) to which we subtractred the weight of the native Lycoming engine, before adding the weight pertaining to all the items considered for the present reconfiguration, assuming some conservative estimates. As apparent, the TOW (take-off weight) is compatible with design requirements, with the added mass being compensated by the missing passenger.

All components have been conveniently arranged as shown in Figure 10, exploiting the space available in the rear fuselage of the Long-EZ. Centre of grav-

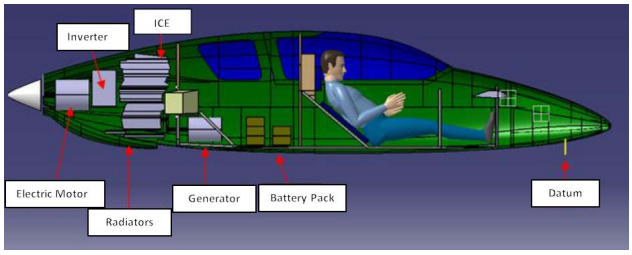

Figure 10. Interior arrangement of the propulsion system components.

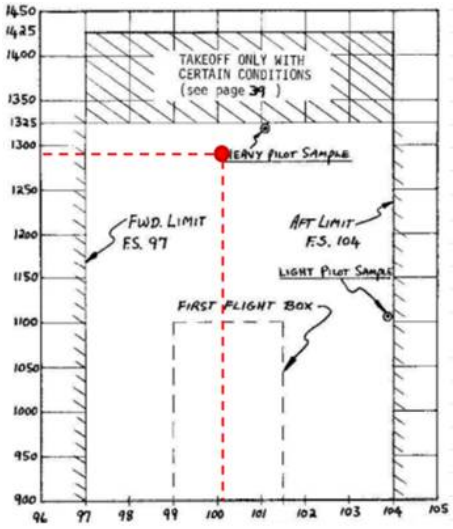

Figure 11. Center of gravity estimation.

ity (CG) position has been evaluated based upon the available data for the Long-EZ model. Figure 11 shows that the estimated CG position falls in the middle of the admissible CG travel as detailed on the Aircraft Flight Manual, thus resulting fully compatible with conventional Long-EZ requirements. Basically, in this reconfiguration, the passenger has been replaced, both in weight and CG position contribution, by the generator and battery pack.

6. Performance Validation

Following the detailed definition of the power system, we updated the aircraft model and checked the fulfilment of our performance goals.

6.1. Performance Goal 1: Maximum airspeed

The first goal of reaching the airspeed of 160 kn in pure electric mode calls for the use of Type 2 cells, because the Peukert effect heavily limits the time of operation of Type 1 cells. In addition, the fuel carried on board is shrinked from the maximum capacity of 65 kg_p to 25 kg_p. In fact, this is enough to fly the mission along the following

Maximum airspeed flight program

i) hybrid take-off and climb to 8,000 ft;

ii) hybrid loiter at 100 kn airspeed for 25 min in order to fully recharge the batteries;

iii) acceleration dash to 160 kn (about 4 min);

iv) upkeep of the airspeed for 15 km.

We remark that this flight program provides for a 20% residual battery charge at the completion of the 15 km segment, in order to guarantee a sound safety margin for descent and landing.

6.2. Performance Goal 2: Time to climb

Also the second goal of reaching 20,000 ft altitude in no more than 20 min was evaluated considering the Type 2 battery pack. Again, the battery capacity degradation due to the Peukert effect does not allow the use of Type 1 cells for the full duration of the mission. In this case, the flight profile is the following

Minimum time-to-climb flight program

i) hybrid take-off and climb to 8,000 ft;

ii) hybrid climb to the target altitude using full ICE power and setting a lower-than-maximum power output for the electric motor (60.5 kW), to optimize the battery discharge rate.

For this climb program, the complete time to 20,000 ft amounts to slightly over 17 min.

6.3. Performance Goal 3: Maximum range

Finally, the third goal of reaching a range of 2,000 km with 80 l of fuel was verified. In this case, embarking the Type 2 battery pack would produce a significant decrease of the maximum fuel embarked, entailing a drastic reduction in range. Therefore, Type 1 batteries were considered in this case. The resulting record flight profile is thus the following

Maximum range flight program

i) hybrid take-off and climb to 8,000 ft;

ii) stepped cruise-climb consisting in 24 alternating segments of pure-electric mode level flight and hybrid mode shallowly climbing flight, up to a final altitude of 11,200 ft.

The distance achieved amounts to 2,380 km. Remarkably, the fuel necessary to fly the same mission with the native propulsive system amounts to 107 l, resulting in no less than 25% fuel saving.

Due to the low current discharge requirement (very close to the nominal one), the Peukert effect has a much lower impact than in the previous performance goal analyses and has been neglected in this case. Concerning mission safety, the final altitude of 11,200 ft allows to fly a very reasonable descent program at an airspeed of 80 kn and a sinking rate of 200 ft/min with very low fuel consumption, without the need for providing additional holding time.

7. Concluding Remarks

We have detailed the preliminary design of a series hybrid reconfiguration for a general aviation airplane. The system appears feasible with the current

technology, easily adaptable to the target aircraft, and capable of supporting the attempt to establish three FAI records for maximum airspeed, time to climb, and maximum range. The analysis of range performance reveals important improvements in fuel efficiency when considering optimal conditions. This may motivate possible extensions to more commercially appealing applications, beyond the present project.

Further developments should address design optimization, detailed component integration, cost analysis, and the conception of an energy management device to aid the pilot. Concurrently, in view of a prototypal realization, an extensive experimental campaign for the propulsive system must be carried out, in order to determine uncertain system parameters, perform hardware integration, study off-design behaviour, and assess global system reliability and safety.

Acknowledgements

The authors gratefully acknowledge informative discussions with colleagues F. Mapelli, R. Viganó, T. Cerri, F. Piscaglia, and C. Gorla (Politecnico di Milano); P. Guglielmi and P. Maggiore (Politecnico di Torino); and with P. Pari (DigiSky Srl).

REFERENCES

1. G. E. Bona, M. Bucari, A. Castagnoli, L. Trainelli, "Flybrid: The Next Step for a Greener Aviation", AIAA paper no. 2014-2733, *Proceedings of the AIAA/3AF Aircraft Noise and Emissions Reduction Symposium, AIAA Aviation and Aeronautics Forum and Exposition 2014*, Atlanta, GA, USA, 2014.
2. G. Romeo, F. Borello, G. Correa, "Setup and test flights of all-electric two-seater aeroplane powered by fuel cells', *Journal of Aircraft*, Vol. 48, pp. 1331-1341, 2011.
3. P. Guglielmi, G. Pellegrino, G. Griva, F. Villata, P. Maggiore, M. Bruno, R. Lamberti, F. Gadrino, "A direct drive solution for Hydrogen supplied all-electric aircraft", *Proceedings of the 35th Conference of the IEEE Industrial Electronics Society IECON 2009*, Porto, Portugal, 2009.
4. A. Nanda, "The propulsive design aspects on the world's first direct drive hybrid airplane", M.Sc. dissertation, Embry-Riddle Aeronautical University, Daytona Beach, USA, 2011.
5. P. Jaenker, F. Anton, "Dimona – The first serial hybrid aircraft", *Proceedings of MEA 2012 – More Electric Aircraft*, Bordeaux, France, 2012.
6. M. Anselmi, S. D'Andrea, "Studio di fattibilitá e progetto preliminare di un sistema propulsivo ibrido per un velivolo leggero (Feasibility study and preliminary design of a hybrid propulsion system for a light airplane)", M.Sc. dissertation (in Italian), Politecnico di Milano, Milano, Italy, 2013.
7. M. Ballarin, "Progetto di un sistema propulsivo ibrido per un velivolo leggero (Design of a hybrid propulsion system for a light airplane)", M.Sc. dissertation (in Italian), Politecnico di Milano, Milano, Italy, 2013.
8. G. Smith, "EAA Air Venture – Oshkosh 2012", *EAA Experimenter*, No. 36, pp. 36–39, 2012.
9. "Certification Specifications for Normal, Utility, Aerobatic and Commuter Aeroplanes CS-23", European Aviation Safety Agency (EASA), Brussels, Belgium, 2012.
10. L. Trainelli, "Range and endurance estimates for serial hybrid aircraft", submitted for publication.
11. D. Doerffel, S. A. Sharkh, "A critical review of using the Peukert equation for determining the remaining capacity of lead-acid and lithium-ion batteries", *Journal of Power Sources*, Vol. 155, pp. 395-400, 2006.